IJEML
An International Journal of Exploratory Meta-Living

Article
www.poisonpie.com/IJEML

An Open Source Journal published through the Auspices of the Poison Pie Publishing House, Knoxville, Tennessee

Editor-in-Chief: Hebeloma Crustuliniforme†

Mission Statement: The purpose of An International Journal of Exploratory Meta-Living is to provide a resource for the dissemination of creative works relevant to the subject of meta-living. The journal welcomes both academic and artistic exercises expressed in any medium capable of being transmitted through the physical mechanisms of the journal. Due consideration also will be given to submissions that do not conform to these mechanisms. The journal explicitly forbids the establishment of a regular publication schedule.

Meta-Living: One useful avenue leading toward an understanding of the term meta-living is through analogy, particularly by considering meta-fiction. Wikipedia, the oracle of all contemporary knowledge, defines meta-fiction as "the literary term describing fictional writing that self-consciously and systematically draws attention to its status as an artifact in posing questions about the relationship between fiction and reality, usually using irony and self-reflection."[1] By straight-forward analogy, meta-living is the existential term describing a manner of living that self-consciously and systematically draws attention to its status as an artifact in posing questions about the relationship between existence and reality, using irony and self-reflection among other devices. These other devices include, but are not limited to, scientific inquiry, ontology, various theologisms, sophistry, rhetoric, tomfoolery, transcendental perspectivism and, of course, the omnipresent specter of post-existential relativism.

[1] https://en.wikipedia.org/wiki/Metafiction, accessed 2014 April 16.

A Note on the Font: This font is Dax Compact Regular, designed by the late Hans Reichel, musician, instrument maker and font designer.

†editor@poisonpie.com

A Materials Perspective on Waterphone Acoustics

Supplementary Information Document

Nicholas S. Carter, Briar K. Faulkner, Bradley J. Straka, Sabrina E. A. Schwerzler and David J. Keffer
Department of Materials Science & Engineering, University of Tennessee, Knoxville, Tennessee, USA

Table of Contents

Table S.1. Complete waterphone parameters

Waterphone Case	Base Case	Small Basin	Steel Rods	Copper Basin
Basin Size	13″	9″	13″	13″
Basin Material	304 SS	304 SS	304 SS	Cu
Basin Material Thickness	0.019″	0.019″	0.019″	0.030
Basin Joining Method	TIG Welding	TIG Welding	TIG Welding	TIG Welding
Number of Rods	36	24	36	36
Smallest Rod Length	2″	2″	2″	2″
Largest Rod Length	10.75″	7.75″	10.5″	10.75″
Rod Length Increments	0.25″	0.25″	0.5″	0.25″
Rod Diameter	3/16″	3/16″	3/16″	3/16″
Rod Materials	Brass	Brass	A36 carbon steel	Brass
Rod Joining Method	Braze	Braze	Braze	Braze
Brazing Filler for Rods	Silver Solder	Silver Solder	Silver Solder	Silver Solder
Pipe Length	15.275″	10.575″	15.275″	15.275″
Pipe Diameter	1.5″	1.5″	1.5″	1.5″
Pipe Material	304 SS	304 SS	304 SS	Cu
Pipe Joining Method	TIG Welding	TIG Welding	TIG Welding	TIG Welding

Table S.2. First 14 fundamental frequencies of the "base case" waterphone.

Creating the Predictive Waterphone Equation					
Length (in)	Length (m)	Calculated	Measured	Constant: 0.128	Constant: 0.130
2.00	0.0508	1006.3	840	795.1	807.5
2.25	0.0572	795.1	618	628.2	638.0
2.50	0.0635	644.0	*432	508.9	516.8
2.75	0.0699	532.3	*440	420.5	427.1
3.00	0.0762	447.2	363	353.4	358.9
3.25	0.0826	381.1	283	301.1	305.8
3.50	0.0889	328.6	254	259.6	263.7
3.75	0.0953	286.2	227	226.2	229.7
4.00	0.1016	251.6	189	198.8	201.9
4.25	0.1080	222.8	178	176.1	178.8
4.50	0.1143	198.8	169	157.1	159.5
4.75	0.1207	178.4	133	141.0	143.2
5.00	0.1270	161.0	127.7	127.2	129.2
5.25	0.1334	146.0	112.7	115.4	117.2
Constants					
Density: 8553 kg/m^3		Diameter: 0.00476 m		Young's Modulus: 97 Gpa	

Table S.3. Stainless steel composition

Energy Dispersive X-ray Spectroscopy (EDXS) of the 304 stainless steel yielded atomic composition. These values are within the tolerance for a typical 304 stainless steel. Phosphorus, sulfur, and carbon are of concentrations below the detection limit of the EDS in use, so experimental values were not recorded.

Element	EDS Atomic Concentration (%)	Standard Composition (%)
Fe	70.42	70.0
Cr	18.78	18.0-20.0
Ni	8.36	8.0-10.5
Mn	1.43	2.0
Si	1.01	0.75
P	-	0.045
S	-	0.030
C	-	0.08

Figure S.1. Waterphone jigs used for fabrication.

Fabrication of a jig was necessary, which was ratcheted to uniformly distribute the rods around the circumference of the basin and included an angled brace to enforce a uniform angle of all the rods relative to the central cylinder. Two jigs were made, one for the 13" basins with 36 rods and another for the 9" basin with 24 rods.

Figure S.2 "Base Case" and "Copper Basin" waterphones.

Figure S.3 Four fabricated waterphones with authors/performers.
(a) "Base Case" played by NSC, (b) "Small Basin" played by SEAS, (c) "Steel Rods" played by BJS, (d) "Copper Basin" played by BKF.

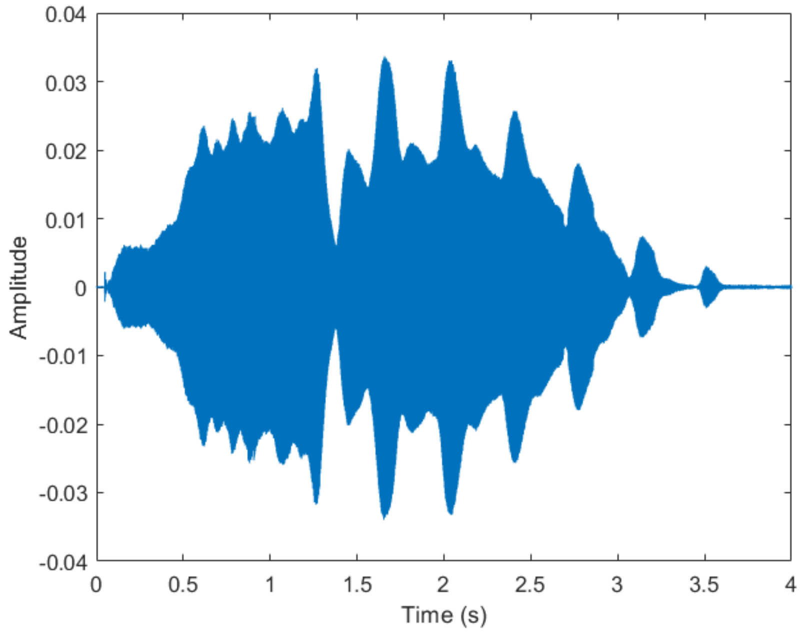

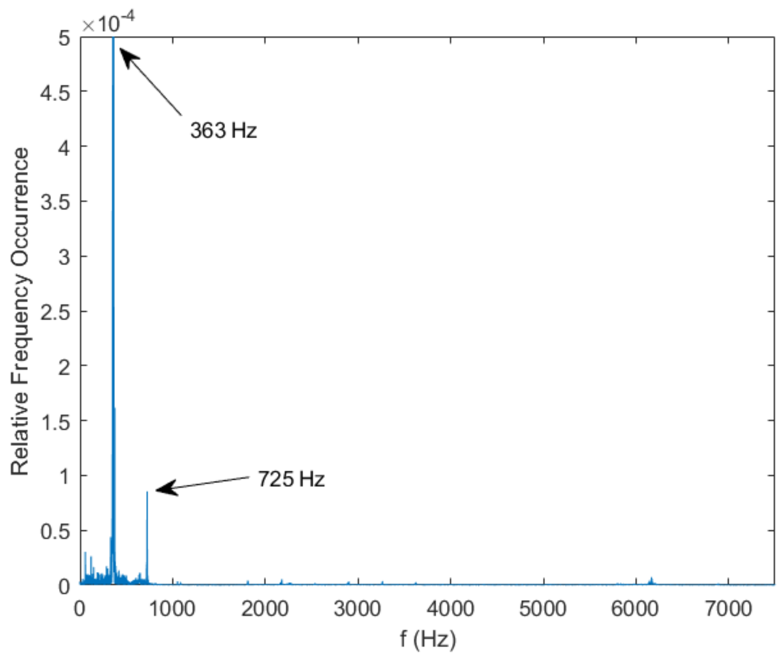

Figure S.4(a) Acoustic characterization of "base case" waterphone without water.
(top) The audio of the three-inch brass rod on the "base case" waterphone without water in the basin. (bottom) The Fourier transform.

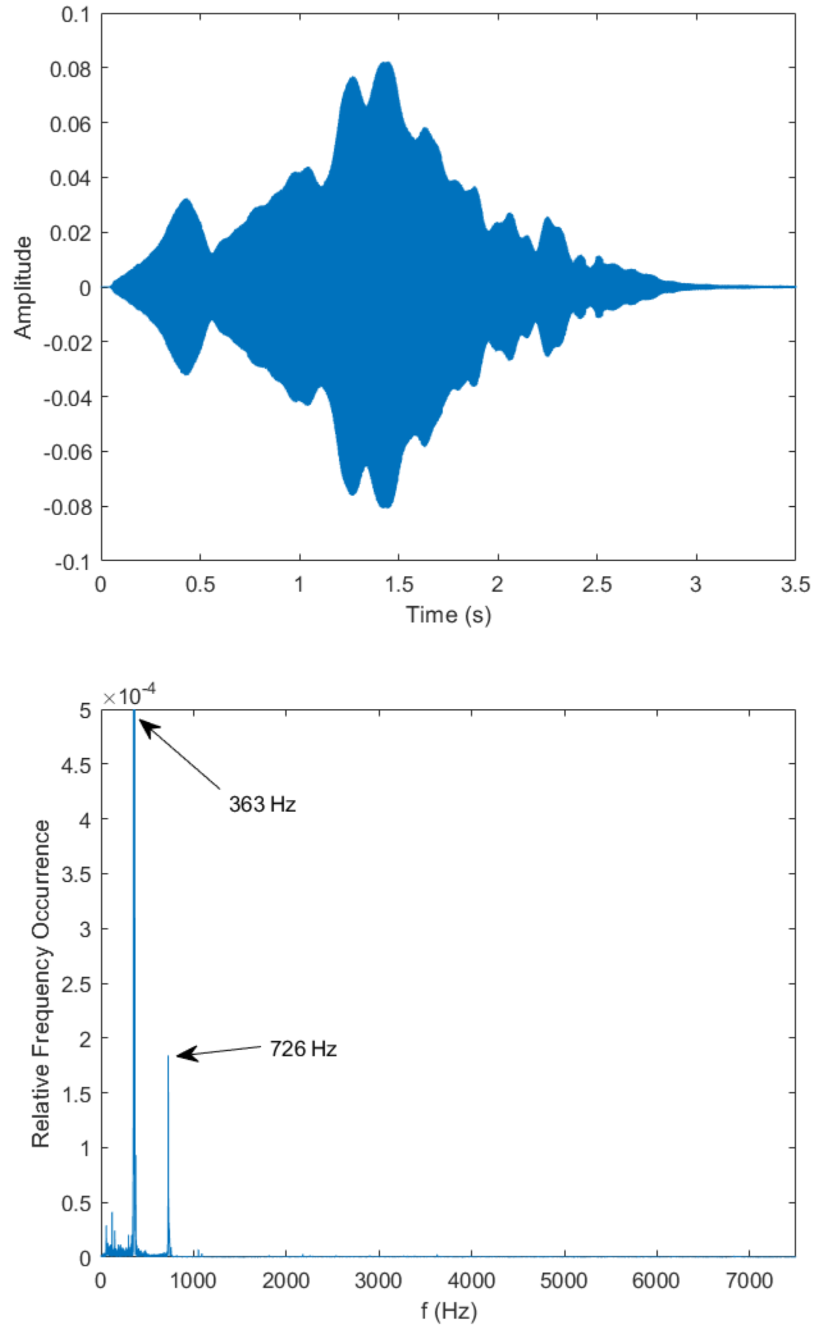

Figure S.4(b) Acoustic characterization of "base case" waterphone with water.
(top) The audio of the three-inch brass rod on the "base case" waterphone with water in the basin. (bottom) The Fourier transform.

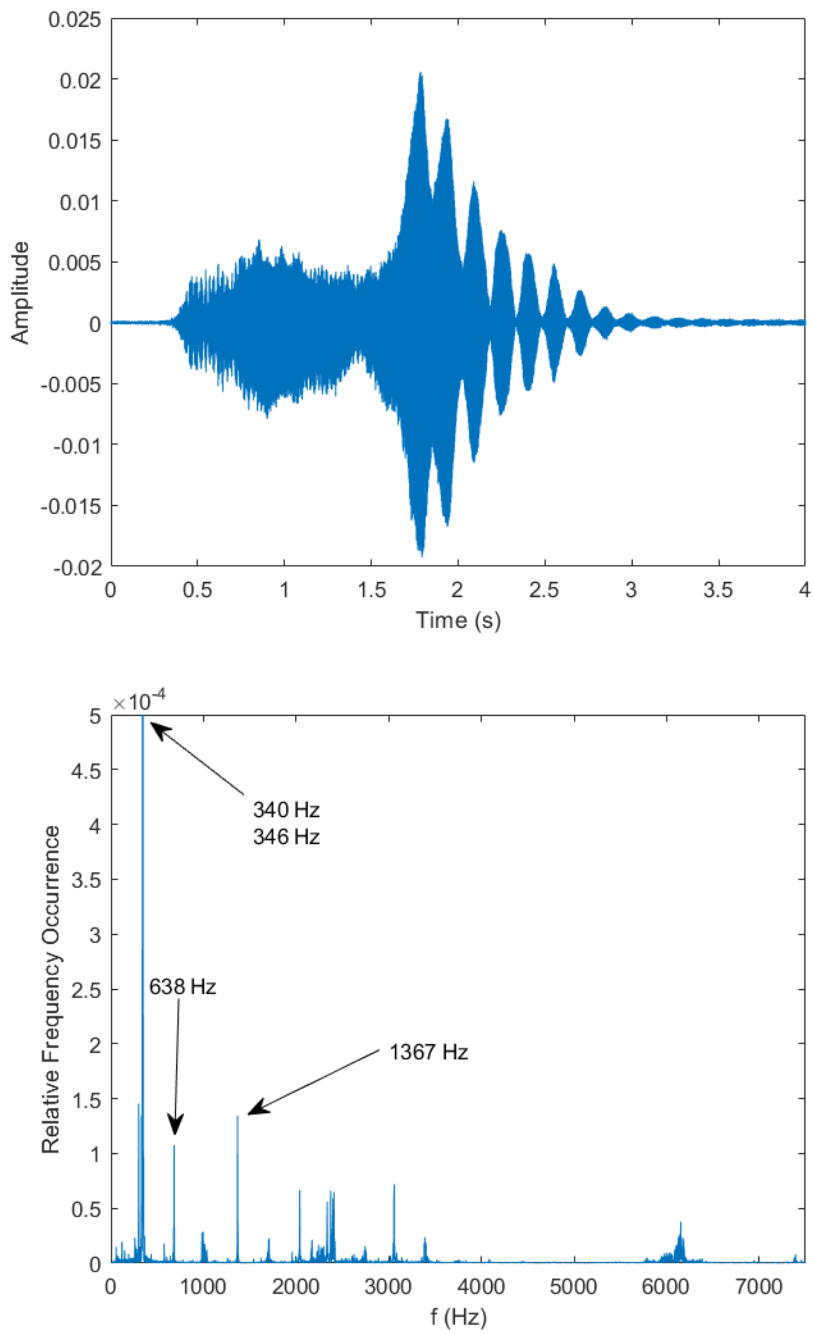

Figure S.4(c) Acoustic characterization of "copper basin" waterphone without water.
(top) The audio of the three-inch brass rod on the "copper basin" waterphone without water in the basin. (bottom) The Fourier transform.

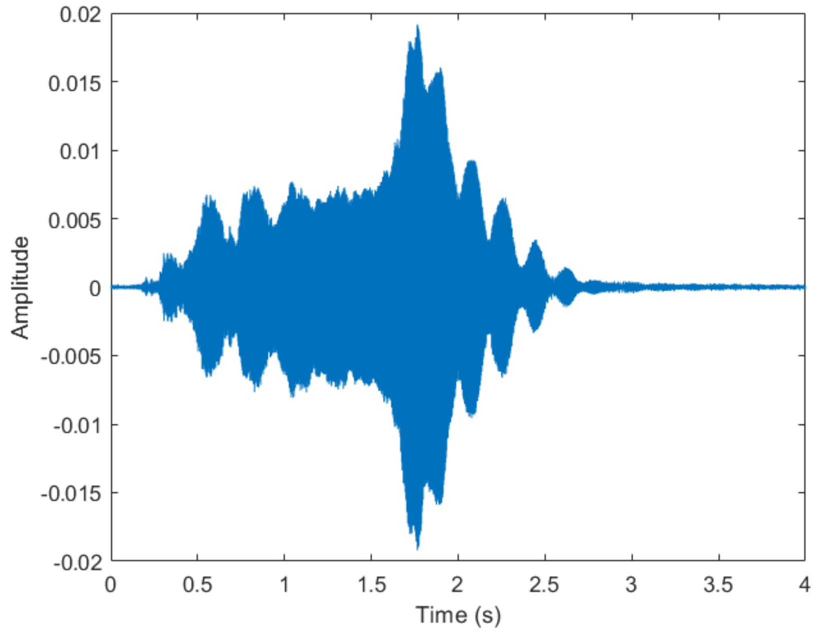

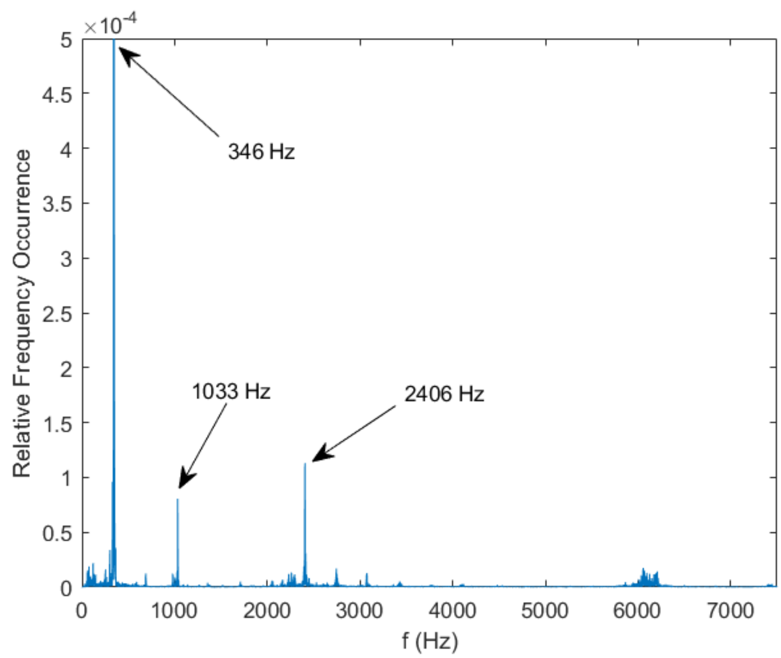

Figure S.4(d) Acoustic characterization of "copper basin" waterphone with water.
(top) The audio of the three-inch brass rod on the "copper basin" waterphone with water in the basin. (bottom) The Fourier transform.

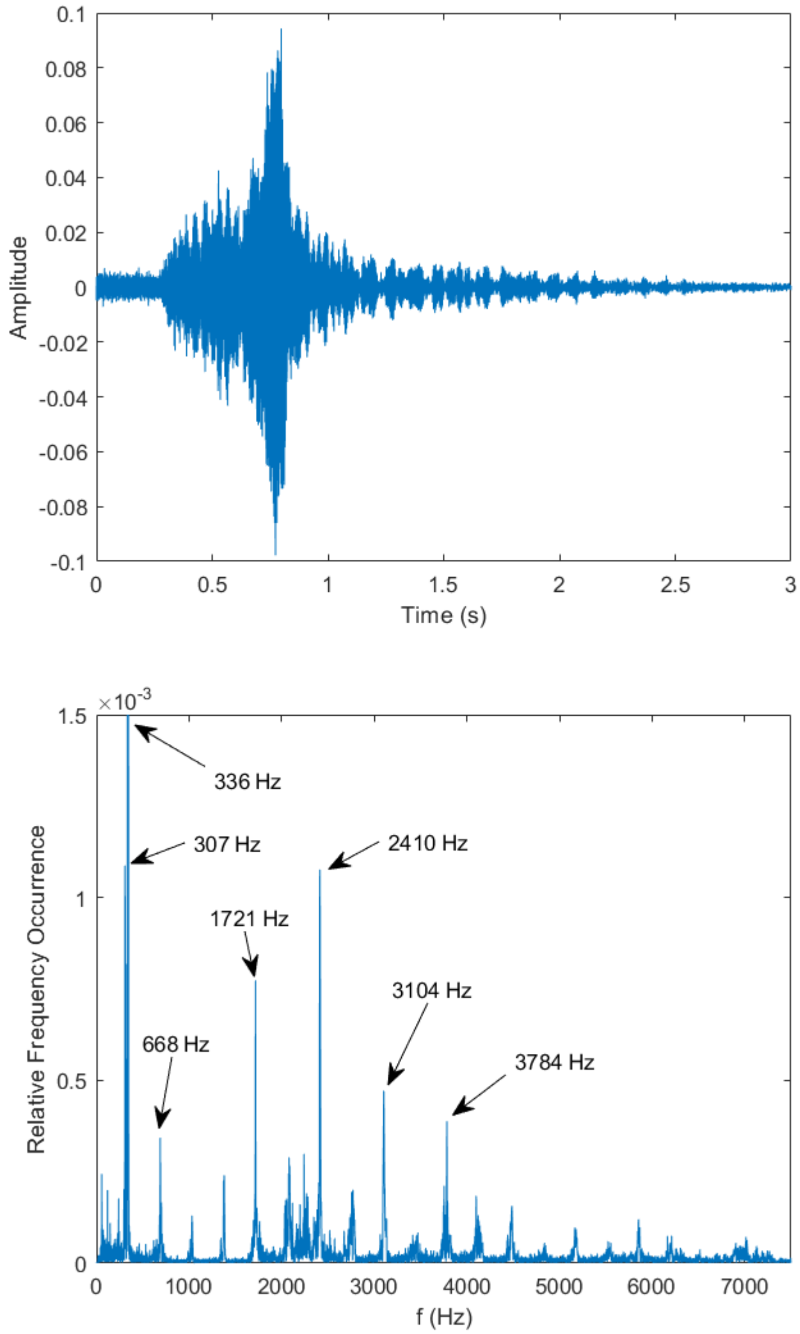

Figure S.4(e) Acoustic characterization of "small basin" waterphone without water.
(top) The audio of the three-inch brass rod on the "small basin" waterphone without water in the basin. (bottom) The Fourier transform.

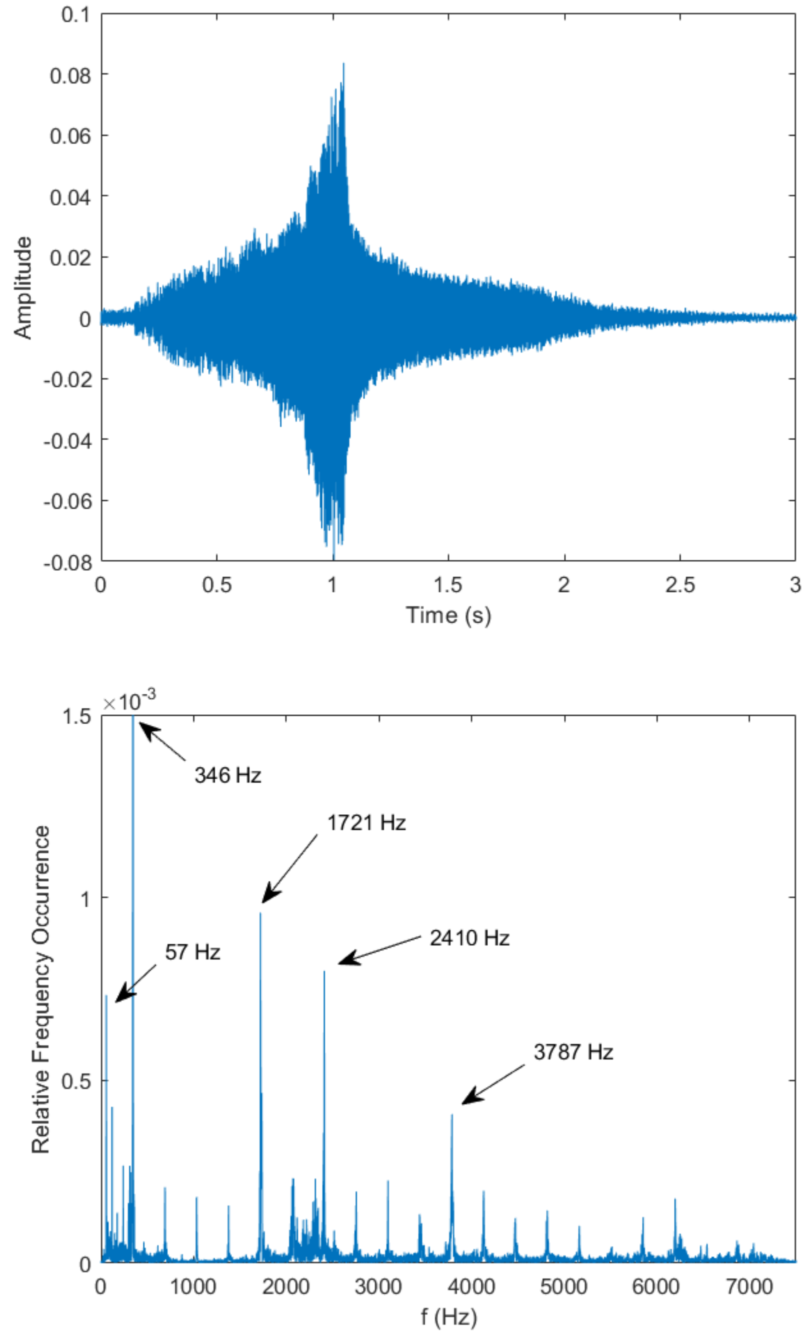

Figure S.4(f) Acoustic characterization of "small basin" waterphone with water.
(top) The audio of the three-inch brass rod on the "small basin" waterphone with water in the basin. (bottom) The Fourier transform.

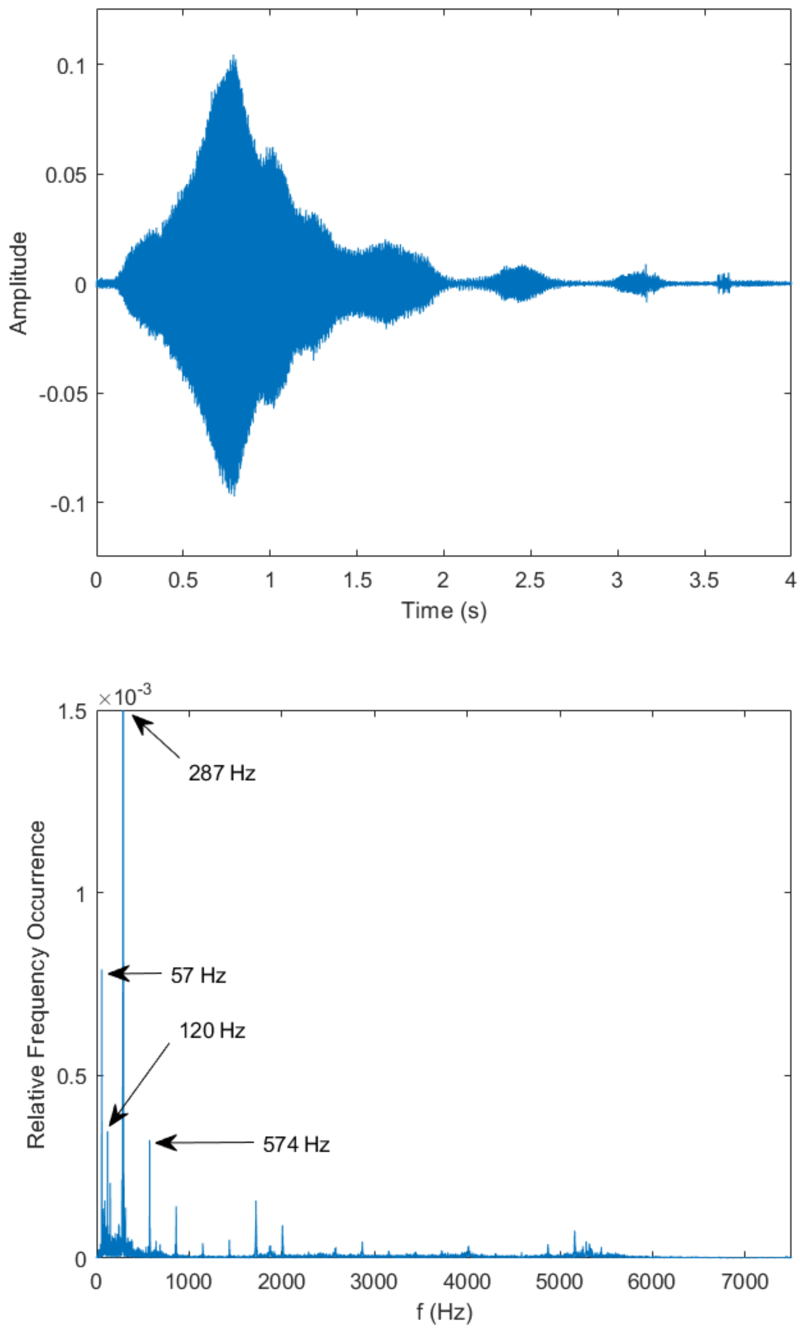

Figure S.4(g) Acoustic characterization of annealed rod on "steel rods" waterphone without water.

(top) The audio of the four-inch annealed rod on the "steel rods" waterphone without water in the basin. (bottom) The Fourier transform.

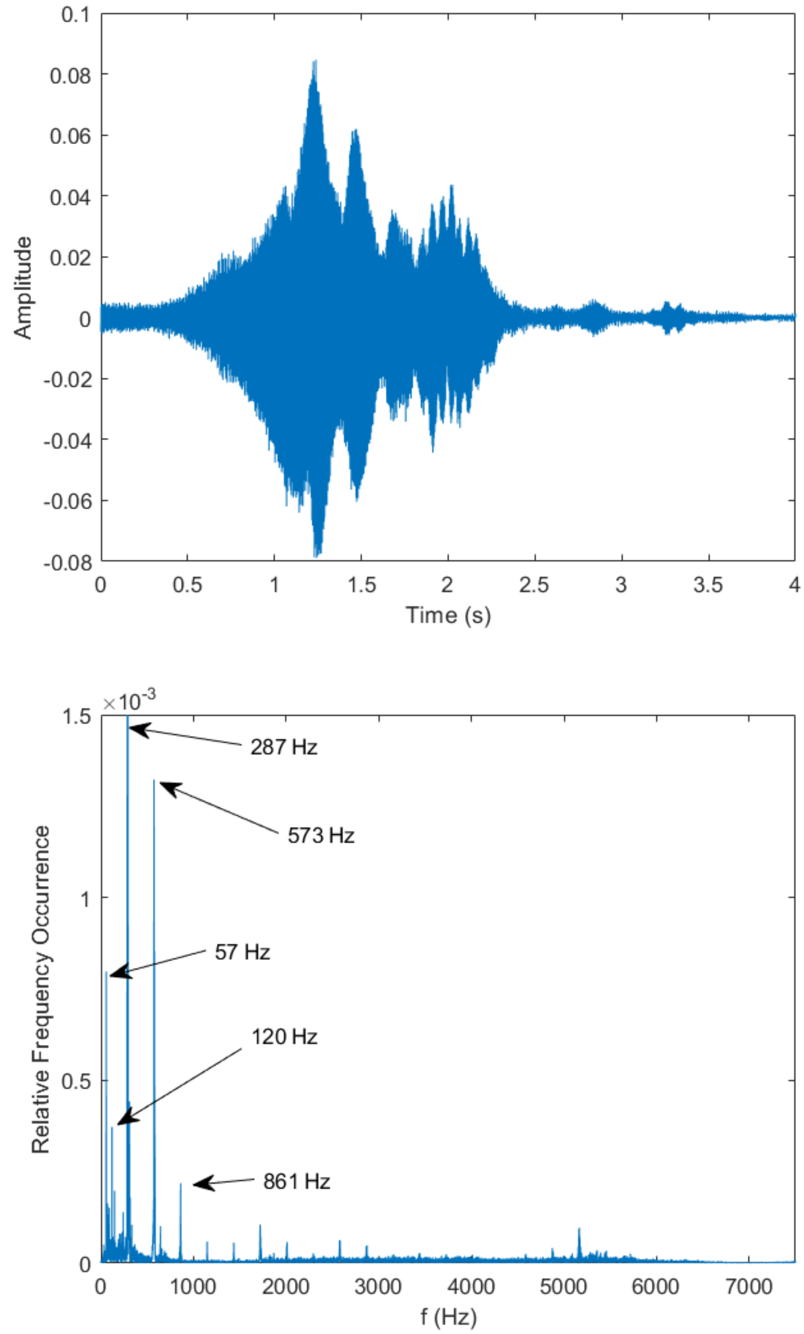

Figure S.4(h) Acoustic characterization of annealed rod on "steel rods" waterphone with water.

(top) The audio of the four-inch annealed rod on the "steel rods" waterphone with water in the basin. (bottom) The Fourier transform.

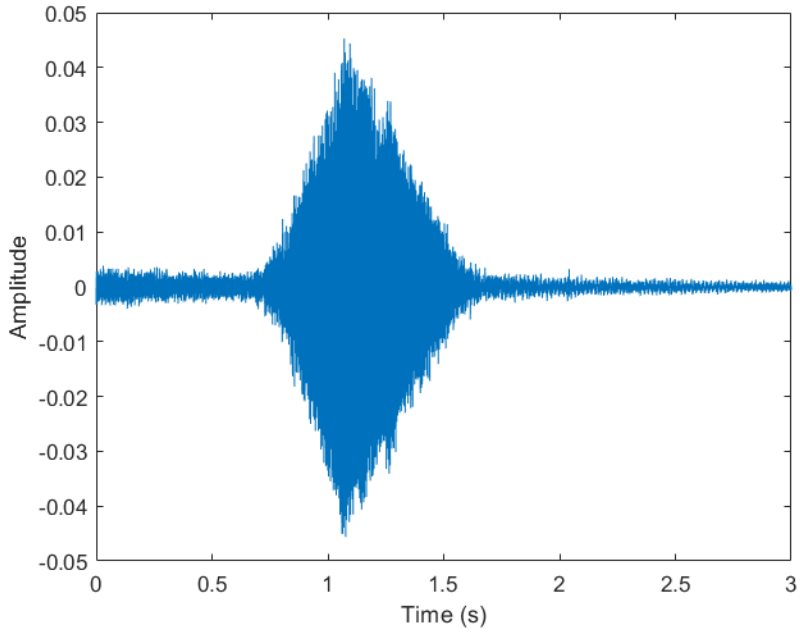

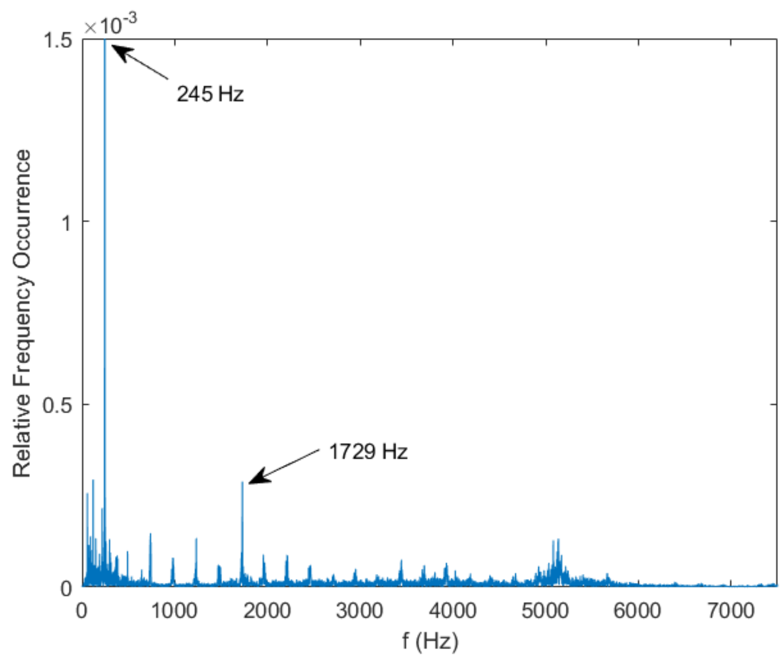

Figure S.4(i) Acoustic characterization of quenched rod on “steel rods” waterphone without water.

(top) The audio of the four-inch quenched rod on the “steel rods” waterphone without water in the basin. (bottom) The Fourier transform.

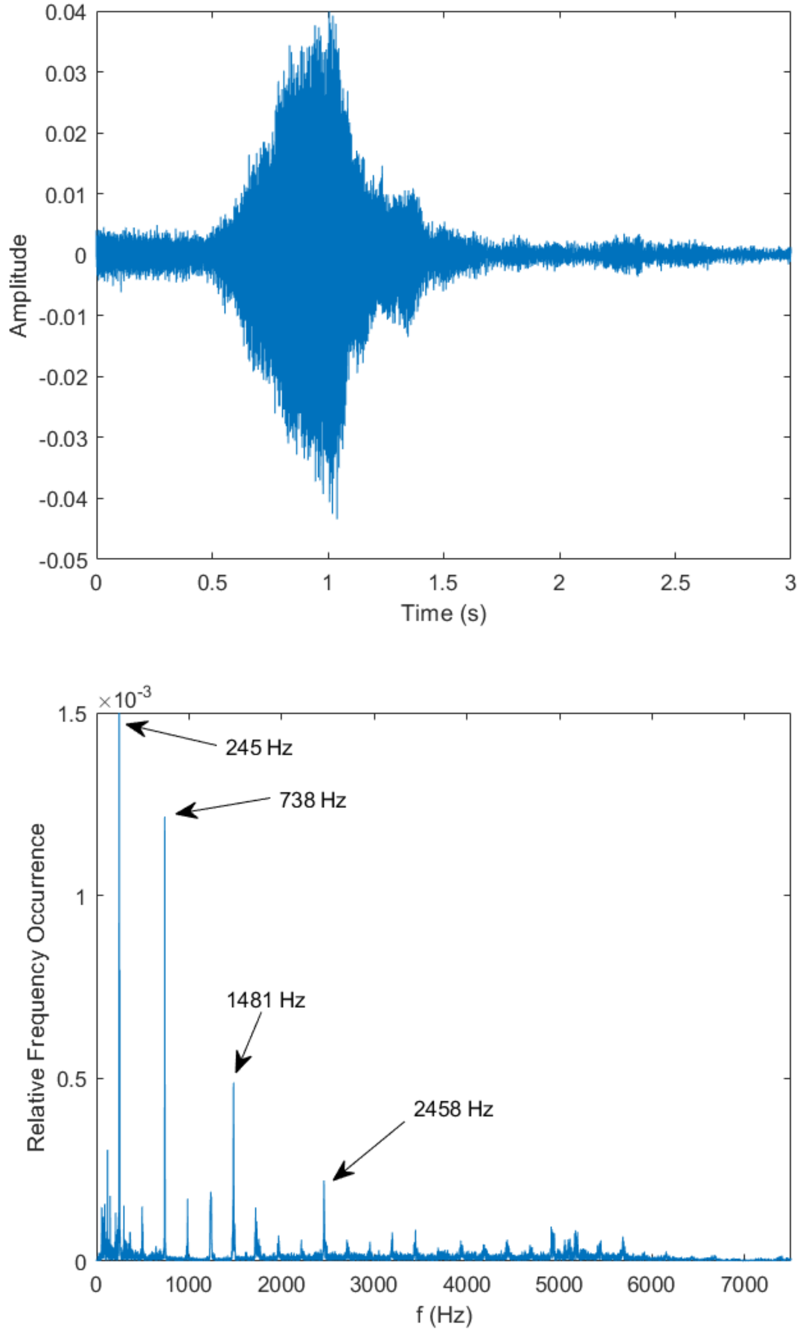

Figure S.4(j) Acoustic characterization of quenched rod on "steel rods" waterphone with water.

(top) The audio of the four-inch quenched rod on the "steel rods" waterphone with water in the basin. (bottom) The Fourier transform.

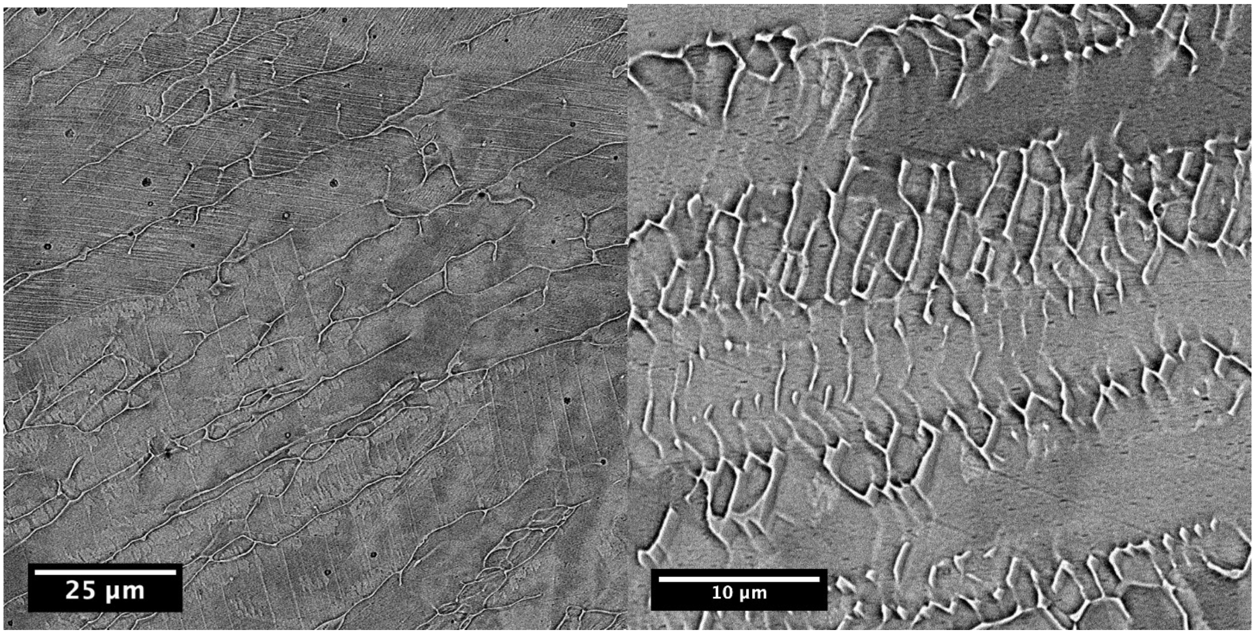

Figure S.5 Electron micrographs of the heat affected zone of the stainless steel weld pool.

The welds performed on the stainless steel instruments were investigated to further understand the heat-effects which are present within the weld pool. Once the etching process was completed Scanning Electron Microscopy (SEM) was performed in order to detect any micro-fissures which may have appeared during welding of the sample. Both the cross-sectioned (left) and flat (right) samples of the weld were examined which gives a higher volume of data as well as revealing the differing heat gradients relative to the sample interface.

The etching process used for stainless steel characterization gives several details which may be evaluated visually. This technique was designed to etch austenitic stainless steel in order to differentiate between ferrite, sigma phase and austenite. The etchant and electrolytic system do this by preferentially etching sigma phase in the sample, while leaving ferrite untouched. This means that ferrite in the HAZ will be a raised area within the sample. Similarly, the etching process performed will heavily etch any sigma phase present, leaving pits or low areas, when inspected. For a 304 autonomous weld, it is expected that neither ferrite nor sigma be in the weld pool, confirming there is no hot cracking or weld embrittlement.

Within the sample in cross-section, shown in Fig. S.4(left), the edge of the weld pool and beginning of the two sides of the coupons may be seen in the bottom left image. In viewing the images and the specific grains shown in the top right, it was concluded that there were no high spots which were above the grain boundaries, thus proving ferrite is absent in the weld. Also, no deep pitting had formed, which rules out sigma phase formation. Lastly, hot cracks were not observed, which the Schaeffler diagram predicts would be the danger of an autonomous 304 weld, thus the cooling rate of the weld was enough for the cross-section to produce no fissures.

As shown in Fig. S.4(right), the flat view of the weld is comparable to the cross-sectioned weld, in that no high or low spots were found. The difference found in the welds is shown by the direction of the dendrites. By evaluating and confirming the welds are solid, with no micro-fissures, it may be concluded that no acoustic loss may be caused by the welding process performed.

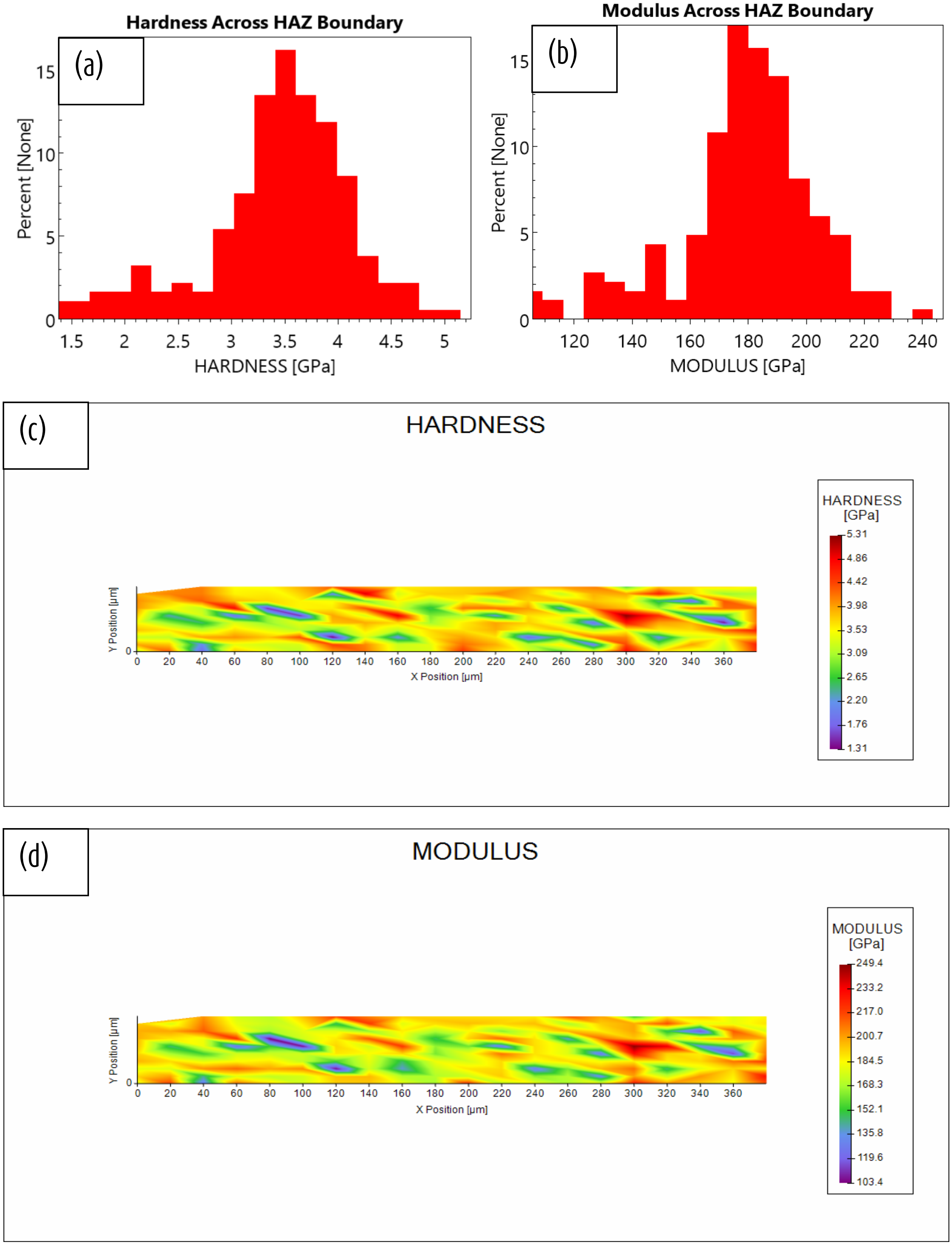
Hardness Across HAZ Boundary
(a)
Percent [None]
0
5
10
15
1.5
2
2.5
3
3.5
4
4.5
5
HARDNESS [GPa]
Modulus Across HAZ Boundary
(b)
Percent [None]
0
5
10
15
120
140
160
180
200
220
240
MODULUS [GPa]
(c)
HARDNESS
Y Position [µm]
X Position [µm]
HARDNESS [GPa]
5.31
4.86
4.42
3.98
3.53
3.09
2.65
2.20
1.76
1.31
(d)
MODULUS
Y Position [µm]
X Position [µm]
MODULUS [GPa]
249.4
233.2
217.0
200.7
184.5
168.3
152.1
135.8
119.6
103.4

Figure S.6 Hardness and Modulus of the heat affected zone of the stainless steel weld pool.

In Fig. S.6, the statistical distribution of hardness (a) and Young's modulus (b) is shown. The corresponding maps of hardness (c) and modulus (d) are also shown. The HAZ of the weld was characterized by nanoindentation. The hardness (left) and elastic modulus (right) are shown. In the mapping data there is a strong relation between tests, which implies testing was configured in a way which befitted the sample. There is a slight variation in both sets of measurements from the reference averages. This difference is slight and has a proposed explanation which may also be seen in the appendix hardness map. It was found that the grain boundaries which were raised due to etching were harder than the base steel. This is depicted as the yellow dendrites in the mapping data. With yellow being the average of the data, it may be inferred that most of the indentations landed on grain boundaries, which have a higher hardness than the stainless steel due to the collection of carbides along those boundaries. This means at small loads; the grain boundaries are much more impactful and raised the overall hardness by approximately 1 GPa from 2.5 to 3.5 GPa. This is not an issue because once a larger load is applied, the effect of the boundaries is lost and the HAZ acts very similar to the base steel.

Modulus data from the mapping shows a trend which increased the average by about 30 GPa from 150 to 180 GPa, which again has been inferred to the carbide formations being tested. The same outlines from grain boundary carbides were found in both maps of the sample. This is consistent with the reference testing which shows a trend downward from low to high loads as the indenter contacts more of the base material. The higher loads show a tendency to favor the overall base material and approach the values measure in the non-HAZ.

The purpose of measuring these characteristics was to cross-analyze the welds in order to ensure there was no embrittlement, as well as characterize the weld for the possibility of developing more complex models for vibrational transfer. The latter being beyond the scope of this project, may be performed later using the reported results.

About The Poison Pie Publishing House

The Poison Pie Publishing House is an independent publisher specializing in post-existential fantasy generated through a non-idiomatic improvisational writing process. In addition to serving as a publishing house, PPPH hosts an arts blog and "An International Journal of Exploratory Meta-Living".